INSTITUTE OF PHYSICS PUBLISHING JOURNAL OF PHYSICS: CONDENSED MATTER

J. Phys.: Condens. Matter **18** (2006) 9525–9540 doi:10.1088/0953-8984/18/41/019

Variational cluster perturbation theory for Bose–Hubbard models

W Koller[1] **and N Dupuis**[1,2]

[1] Department of Mathematics, Imperial College, 180 Queen's Gate, London SW7 2AZ, UK
[2] Laboratoire de Physique des Solides, CNRS UMR 8502, Université Paris-Sud, 91405 Orsay, France

Received 17 July 2006, in final form 12 September 2006
Published 29 September 2006
Online at stacks.iop.org/JPhysCM/18/9525

Abstract

We discuss the application of the variational cluster perturbation theory (VCPT) to the Mott-insulator-to-superfluid transition in the Bose–Hubbard model. We show how the VCPT can be formulated in such a way that it gives a translation invariant excitation spectrum—free of spurious gaps—despite the fact that it formally breaks translation invariance. The phase diagram and the single-particle Green function in the insulating phase are obtained for one-dimensional systems. When the chemical potential of the cluster is taken as a variational parameter, the VCPT reproduces the dimensional dependence of the phase diagram even for one-site clusters. We find a good quantitative agreement with the results of the density-matrix renormalization group when the number of sites in the cluster becomes of order 10. The extension of the method to the superfluid phase is discussed.

(Some figures in this article are in colour only in the electronic version)

1. Introduction

The Bose–Hubbard model describes interacting bosons on a lattice. It provides a generic description of the quantum phase transition between superfluid (SF) and Mott-insulator (MI) states observed in condensed-matter systems such as Josephson junction arrays or granular superconductors [1], as well as in ultracold atoms in optical lattices [2–5]. The remarkable degree of experimental control over all the relevant parameters (density, interaction strength, lattice geometry and dimensionality) in ultracold atoms makes possible a detailed study of the MI–SF transition.

The Bose–Hubbard model has been studied numerically using the Gutzwiller mean-field ansatz [6–8], the density-matrix renormalization group [9, 10], exact diagonalizations [11, 12] and quantum Monte Carlo [13–15]. (More recent works include the harmonic trap potential that confines the ultracold atomic gases; see for instance [16].) Most analytical approaches rely on a perturbation theory that assumes the kinetic energy to be small and treats the on-site

repulsion exactly. Intersite hopping is taken into account either at the mean-field level or in perturbation in a strong-coupling expansion [1, 17–27].

In this paper, we apply the variational cluster perturbation theory (VCPT) to the Bose–Hubbard model at commensurate density. The VCPT has been developed for strongly correlated fermion systems. It is an extension of cluster perturbation theory (CPT) that is based on the self-energy functional approach (SFA). Within the CPT [28–30], the lattice is partitioned into disconnected identical clusters. The Hamiltonian of the cluster is solved numerically, and the intercluster hopping is then treated perturbatively to leading order in a strong-coupling expansion. Contrary to exact diagonalizations of small systems, the CPT provides results in the thermodynamic limit, and the single-particle Green function is defined for any wavevector in the Brillouin zone. When based on a single-site cluster, the CPT yields the Hubbard I approximation [31]; applied to bosonic systems, it reproduces the leading order of the aforementioned strong-coupling theory [23].

The SFA is based on the variational principle $\delta\Omega[\Sigma]/\delta\Sigma = 0$ for the grand potential expressed as a functional of the self-energy Σ [32–34]. The stationary condition is solved within a restricted space of self-energies taken from a reference system that can be solved numerically. Within the VCPT [34, 35], the reference system consists of disconnected identical clusters. The VCPT improves on the CPT since the parameters of the intracluster kinetic Hamiltonian are variational. In particular, this enables us to consider broken-symmetry states. The VCPT has been used with some success to study strongly correlated electron systems [35–39].

The outline of the paper is as follows. In section 2, we describe the SFA and the VCPT for bosonic models in the absence of superfluidity. We modify the original formulation of the SFA [32] to ensure that final results remain translation invariant regardless of the choice of reference system. We also stress the necessity to consider the chemical potential of the cluster as a variational parameter. In section 3, we present numerical results for the phase diagram and the single-particle Green function in a one-dimensional (1D) system. Even in the simplest case of a reference system consisting of single-site clusters, the VCPT improves drastically on the CPT. In particular, we obtain the correct form of the Mott lobes in the $(t/U, \mu/U)$ phase diagram (t is the hopping amplitude, U the onsite repulsion and μ the chemical potential). We find a good quantitative agreement with the results of the density-matrix renormalization group [10] when the number of sites in the cluster becomes of order 10. The last section is devoted to a summary of our results and a discussion of future developments, in particular the extension of the VCPT to the superfluid phase.

2. Variational cluster perturbation theory for bosons

The Bose–Hubbard model is defined by the Hamiltonian

$$H = -\sum_{\mathbf{r},\mathbf{r}'}(\psi^\dagger_{\mathbf{r}} t_{\mathbf{r}\mathbf{r}'}\psi_{\mathbf{r}'} + \text{H.c.}) - \mu\sum_{\mathbf{r}} n_{\mathbf{r}} + \frac{U}{2}\sum_{\mathbf{r}} n_{\mathbf{r}}(n_{\mathbf{r}} - 1), \tag{1}$$

where $\psi_{\mathbf{r}}$, $\psi^\dagger_{\mathbf{r}}$ are annihilation/creation bosonic operators and $n_{\mathbf{r}} = \psi^\dagger_{\mathbf{r}}\psi_{\mathbf{r}}$. The discrete variable $\mathbf{r}$ labels the sites of the lattice, which is assumed to be bipartite with coordination number z. The hopping matrix $\hat{t}$ satisfies $t_{\mathbf{r}\mathbf{r}'} = t > 0$ if $\mathbf{r}$ and $\mathbf{r}'$ are nearest neighbours and vanishes otherwise; this assumption can, however, be easily relaxed and longer-range hopping considered. For reasons explained below, the boson–boson interaction should be onsite. The density n, i.e. the average number of bosons per site, is fixed by the chemical potential μ. In the following, we shall consider only the Mott phase and the zero-temperature limit.

2.1. General formalism

In the absence of superfluidity ($\langle\psi_{\mathbf{r}}\rangle = 0$), the grand potential (per lattice site) Ω and the single-particle Green function G can be obtained from the stationary point of the functional [40–42]

$$\Omega[G] = \frac{1}{N\beta}\left\{\mathrm{Tr}\ln(-G^{-1}) + \mathrm{Tr}(G_0^{-1}G - 1) + \Phi[G]\right\}, \tag{2}$$

where G_0 is the non-interacting Green function and $\Phi[G]$ the Luttinger–Ward functional. $\beta = 1/T$ is the inverse temperature and N the number of lattice sites. Tr denotes a trace over space and time indices. The stationary condition $\delta\Omega[G]/\delta G = 0$ yields the Dyson equation

$$G^{-1} = G_0^{-1} - \Sigma, \tag{3}$$

where the self-energy Σ is defined by

$$\Sigma_{ij} = -\frac{\delta\Phi[G]}{\delta G_{ji}}. \tag{4}$$

i and j are collective indices that label position and time.

The SFA is based on the functional [32]

$$\Omega[\Sigma] = \frac{1}{N\beta}\left\{\mathrm{Tr}\ln(-G_0^{-1} + \Sigma) + F[\Sigma]\right\}, \tag{5}$$

where

$$F[\Sigma] = \Phi[G] + \mathrm{Tr}(\Sigma G) \tag{6}$$

is the Legendre transform of $\Phi[G]$. In equation (6), G should be considered as a functional $G[\Sigma]$ of the self-energy obtained by inverting (4). F satisfies

$$\frac{\delta F[\Sigma]}{\delta\Sigma_{ij}} = G_{ji}, \tag{7}$$

and the stationary condition $\delta\Omega[\Sigma]/\delta\Sigma = 0$ reproduces the Dyson equation (3).

So far, we have followed the approach of [32] with minor modifications due to the fact that we consider bosons instead of fermions. We now introduce a refinement of the approach, the motivation for which will be discussed below. In a translation-invariant system, the actual self-energy is diagonal in $\mathbf{k}$ space: $\Sigma(\mathbf{k}, \mathbf{k}', z) = \delta_{\mathbf{k},\mathbf{k}'}\Sigma(\mathbf{k}, \mathbf{k}, z)$ (z is a complex frequency). Without changing its value at the stationary point, we can therefore modify the functional (5) into

$$\Omega[\Sigma] = \frac{1}{N\beta}\left\{\mathrm{Tr}\ln(-G_0^{-1} + \tilde{\Sigma}) + F[\Sigma]\right\}, \tag{8}$$

where

$$\tilde{\Sigma}(\mathbf{k}, \mathbf{k}', z) = \delta_{\mathbf{k},\mathbf{k}'}\Sigma(\mathbf{k}, \mathbf{k}, z) \tag{9}$$

is the diagonal part of the self-energy. One easily verifies that the stationary condition $\delta\Omega[\Sigma]/\delta\Sigma = 0$ yields the Dyson equation

$$G^{-1}(\mathbf{k}, z) = G_0^{-1}(\mathbf{k}, z) - \tilde{\Sigma}(\mathbf{k}, z), \tag{10}$$

where $G_0^{-1}(\mathbf{k}, z) = z + \mu - \epsilon_{\mathbf{k}}$. $\epsilon_{\mathbf{k}}$ is the Fourier transform of $-t_{\mathbf{r},\mathbf{r}'}$ and gives the lattice dispersion of the bosons. In equation (10), $\tilde{\Sigma}(\mathbf{k}, z)$ denotes $\tilde{\Sigma}(\mathbf{k}, \mathbf{k}, z)$, etc. Thus the two functionals (5) and (8) contain the same information in the case of translation invariant systems.

Let us now consider the two Hamiltonians [32]

$$H(x) = H_0(x) + H_{\mathrm{U}}, \qquad H(x') = H_0(x') + H_{\mathrm{U}}. \tag{11}$$

$H(x)$ is the Hamiltonian of the Bose–Hubbard model (equation (1)), and $H(x')$ that of a reference system. Both Hamiltonians are defined on the same lattice and share the same interaction Hamiltonian $H_{\rm U}$. The kinetic parts $H_0(x)$ and $H_0(x')$ include a chemical potential term. x stands for the parameters on which H_0 depends: the intersite hopping matrix $\hat{t}$ and the chemical potential μ. The Hamiltonian $H(x)$ is translation invariant, but that of the reference system, $H(x')$, may not be. The Luttinger–Ward functional $\Phi[G]$ is given by the sum of the two-particle irreducible (skeleton) diagrams [41, 42] and is independent of G_0. It follows that $H(x)$ and $H(x')$ share the same Luttinger–Ward functional $\Phi[G]$ and therefore the same functional $F[\Sigma]$ [32]. This leads us to consider the functionals

$$\begin{aligned}\Omega_x[\Sigma] &= \frac{1}{N\beta}\left\{\mathrm{Tr}\ln(-G_0^{-1}+\tilde{\Sigma}) + F[\Sigma]\right\},\\ \Omega_{x'}[\Sigma] &= \frac{1}{N\beta}\left\{\mathrm{Tr}\ln(-G_0'^{-1}+\Sigma) + F[\Sigma]\right\},\end{aligned} \tag{12}$$

where $G_0 \equiv G_0(x)$ and $G_0' \equiv G_0(x')$ are the Green functions corresponding to $H_0(x)$ and $H_0(x')$, respectively. Note that we have taken advantage of the translation invariance of $H(x)$ in writing $\Omega_x[\Sigma]$. The unknown functional $F[\Sigma]$ can now be eliminated by taking the difference of the two preceding equations,

$$\Omega_x[\Sigma] = \Omega_{x'}[\Sigma] + \frac{1}{N\beta}\left\{\mathrm{Tr}\ln(-G_0^{-1}+\tilde{\Sigma}) - \mathrm{Tr}\ln(-G_0'^{-1}+\Sigma)\right\}. \tag{13}$$

The form (13) of the self-energy functional $\Omega_x[\Sigma]$ is exact. To make the determination of the stationary points of $\Omega_x[\Sigma]$ possible, one has to restrict the space of self-energies. A natural approximation is to evaluate $\Omega_x[\Sigma]$ for the (physical) self-energies $\Sigma(x')$ obtained from the reference system—assuming that the reference Hamiltonian can be solved exactly [32]. The functional $\Omega_x[\Sigma(x')] \equiv \Omega_x(x')$ becomes a function of x',

$$\Omega_x(x') = \Omega' + \frac{1}{N\beta}\left\{\mathrm{Tr}\ln[-G_0^{-1}+\tilde{\Sigma}(x')] - \mathrm{Tr}\ln[-G_0'^{-1}+\Sigma(x')]\right\} \tag{14}$$

where $\Omega' = \Omega_{x'}[\Sigma(x')]$ is the exact grand potential of the reference system. The stationary condition becomes

$$\frac{\partial\Omega_x(x')}{\partial x'} = 0. \tag{15}$$

Note that the stationary point does not have to be a minimum. We shall see that it is actually never a minimum when the chemical potential of the reference system is taken as a variational parameter. This conclusion also holds in fermion systems [38].

2.2. Reference system

In the VCPT one considers a reference system consisting of a superlattice of $N_{\rm c} = N/L$ identical clusters with no intercluster kinetic coupling (L is the number of sites in a cluster). The determination of Ω' and the self-energy $\Sigma(x')$ then requires us to solve a finite size system Hamiltonian provided that the interaction is local. For moderate values of L this can be done numerically. Equation (14) can be rewritten as

$$\Omega_x(x') = \Omega' - \frac{1}{N\beta}\sum_{\mathbf{k},\omega_n}\ln[-G(\mathbf{k},\mathrm{i}\omega_n)]\mathrm{e}^{\mathrm{i}\omega_n\eta} + \frac{1}{N\beta}\sum_{\omega_n}\mathrm{tr}\ln[-G'(\mathrm{i}\omega_n)]\mathrm{e}^{\mathrm{i}\omega_n\eta} \tag{16}$$

(ω_n is a bosonic Matsubara frequency), where $G^{-1} = G_0^{-1} - \tilde{\Sigma}$ and $G'^{-1} = G_0'^{-1} - \Sigma$ (from now on, we do not write explicitly the x' dependence of $\Sigma(x')$). tr denotes the trace over space indices. tr $\ln(-G')$ can be evaluated by considering a single cluster and multiplying the result

by $N_c = N/L$ to take into account the total number of clusters. When the chemical potentials μ and μ' differ, the usual factor $e^{i\omega_n\eta}$ ($\eta \to 0^+$) is necessary for the sum over ω_n to converge.

Let us now discuss the motivation for using the functional (8) rather than (5). The reference system has the periodicity of the cluster superlattice, but not that of the translation-invariant system of interest. Except for single-site clusters, the self-energy Σ is not diagonal in $\mathbf{k}$ space. By making use of the functional (8), we ensure the translation invariance of the Green function defined by equation (10). In applications of the VCPT to fermionic systems, the translation-invariant Green function of the system was approximated by the diagonal part of $G = (G_0^{-1} - \Sigma)^{-1}$. However, because Σ itself is not translation invariant, the resulting excitation spectrum exhibits spurious gaps that reflect the periodicity of the reference system. To some extent, this difficulty can be eliminated by introducing an artificial broadening of the energy states; technically this is achieved by choosing a sufficiently large value of η. In bosonic systems, even when one allows for an energy broadening, these gaps are so pronounced that the excitation spectrum does not bear much physical meaning.

The translation-invariant self-energy $\tilde{\Sigma}(\mathbf{k}, z)$ turns out to be simply related to the cluster self-energy when periodic boundary conditions—as allowed in the VCPT, since this simply assumes a particular choice of the (in principle variational) intersite hopping matrix $\hat{t}'$—are chosen for the cluster. Let us write the self-energy of the reference system as

$$\Sigma(\mathbf{R} + \mathbf{r}_a, \mathbf{R}' + \mathbf{r}_b, z) = \delta_{\mathbf{R},\mathbf{R}'}\Sigma_{ab}(z), \tag{17}$$

where $\Sigma_{ab}(z)$ is the cluster self-energy obtained by numerically solving the Hamiltonian $H(x')$. We use the notation $\mathbf{R} + \mathbf{r}_a$ for a site of a lattice, $\mathbf{R}$ for a site of the superlattice, and $\mathbf{r}_a$ ($a \in [1, L]$) for the position within the cluster. The translation-invariant self-energy then reads

$$\tilde{\Sigma}(\mathbf{k}, z) = \frac{1}{L}\sum_{a,b=1}^{L} e^{-i\mathbf{k}\cdot(\mathbf{r}_a - \mathbf{r}_b)}\Sigma_{ab}(z). \tag{18}$$

With periodic boundary conditions for the cluster, we can define the Fourier transform of $\Sigma_{ab}(z)$ for any vector $\mathbf{k}$ of the reciprocal superlattice. In that case, $\tilde{\Sigma}(\mathbf{k}, z)$ defined by equation (18) is nothing but the interpolation of the translation-invariant cluster self-energy to all vectors $\mathbf{k}$ of the Brillouin zone.

2.3. Numerical implementation

To numerically evaluate the sum over Matsubara frequencies in equation (16), one has to get rid of the convergence factor $e^{i\omega_n\eta}$. To this end, one subtracts and adds the term

$$\frac{1}{\beta N}\sum_{\mathbf{K},\omega_n} \mathrm{tr}_c \ln\left[1 - \frac{\Delta h_0(\mathbf{K})}{i\omega_n - y}\right] e^{i\omega_n\eta} = \frac{1}{\beta N}\sum_{\mathbf{K},\alpha} \ln\left[1 - e^{-\beta(y+\lambda_\alpha(\mathbf{K}))}\right] - \frac{1}{\beta}\ln\left(1 - e^{-\beta y}\right), \tag{19}$$

where tr_c denotes the trace over intracluster space indices. $\Delta h_0 = h_0 - h_0'$ is defined from the Green functions $G_0^{-1}(i\omega_n) = i\omega_n - h_0$ and $G_0'^{-1}(i\omega_n) = i\omega_n - h_0'$. $\Delta h_0(\mathbf{K})$ is the Fourier transform of Δh_0 with respect to the superlattice of clusters,

$$\Delta h_0(\mathbf{K})_{ab} = \sum_{\mathbf{R}} e^{-i\mathbf{K}\cdot(\mathbf{R}-\mathbf{R}')}\Delta h_0(\mathbf{R} + \mathbf{r}_a, \mathbf{R}' + \mathbf{r}_b). \tag{20}$$

$\Delta h_0(\mathbf{r}, \mathbf{r}')$ denotes the matrix elements of Δh_0 in real space, and $\mathbf{K}$ is a vector of the reduced Brillouin zone corresponding to the superlattice. $\lambda_\alpha(\mathbf{K})$ ($\alpha \in [1, L]$) are the eigenvalues of $\Delta h_0(\mathbf{K})$, and the real number y should satisfy $y > \max_{\alpha,\mathbf{K}} |\lambda_\alpha(\mathbf{K})|$. Equation (19) is derived

in appendix A. Combining (16) and (19), we finally obtain

$$\Omega_x(x') = \Omega' - \frac{1}{N\beta}\sum_{\omega_n}\left\{\sum_{\mathbf{k}}\ln[-G(\mathbf{k},\mathrm{i}\omega_n)] - \mathrm{tr}\ln[-G'(\mathrm{i}\omega_n)] + \sum_{\mathbf{K}}\mathrm{tr}_c\ln\left[1-\frac{\Delta h_0(\mathbf{K})}{\mathrm{i}\omega_n - y}\right]\right\}$$
$$+\frac{1}{\beta N}\sum_{\mathbf{K},\alpha}\ln\left[1-\mathrm{e}^{-\beta(y+\lambda_\alpha(\mathbf{K}))}\right] - \frac{1}{\beta}\ln\left(1-\mathrm{e}^{-\beta y}\right). \tag{21}$$

The term inside the curly brackets behaves as $1/\omega_n^2$ when $|\omega_n| \to \infty$, so that the convergence factor $\mathrm{e}^{\mathrm{i}\omega_n\eta}$ is no longer necessary. Equation (21) is the starting point of the numerical calculations discussed in section 3.

2.4. μ' as a variational parameter

In this section we discuss the role of the chemical potential μ' of the cluster as a variational parameter. The boson density is obtained from

$$n = -\frac{\partial\Omega_x(x')}{\partial\mu}, \tag{22}$$

where the value of $x' = x'(x)$ is determined from the stationary condition (15). Combining equations (22) and (15), we obtain

$$n = -\left.\frac{\partial\Omega_x(x')}{\partial\mu}\right|_{x'} - \left.\frac{\partial\Omega_x(x')}{\partial x'}\right|_{x}\frac{\partial x'}{\partial\mu} = -\left.\frac{\partial\Omega_x(x')}{\partial\mu}\right|_{x'}. \tag{23}$$

From equation (16), we then deduce

$$n = -\frac{\partial}{\partial\mu}\frac{1}{N\beta}\sum_{\mathbf{k},\omega_n}\ln[-G^{-1}(\mathbf{k},\mathrm{i}\omega_n)]\mathrm{e}^{\mathrm{i}\omega_n\eta}\Big|_{x'}$$
$$= -\frac{1}{N\beta}\mathrm{Tr}(G). \tag{24}$$

Here we have used the fact that the only dependence on μ (at fixed x') comes from $G_0(\mathbf{k},\mathrm{i}\omega_n)$. Thus the stationary condition (15) ensures that the approach is thermodynamically consistent: the boson density can be calculated either from the grand potential or the single-particle Green function.

The stationary condition also ensures that the boson density n of the system is the same as that of the reference system (n_c). To see this, we make use of the following result derived in appendix B:

$$\sum_{\mathbf{k},\omega_n}\ln[-G(\mathbf{k},\mathrm{i}\omega_n)]\mathrm{e}^{\mathrm{i}\omega_n\eta} = -\sum_{\mathbf{k},\gamma}\ln\left|1-\mathrm{e}^{-\beta E_\gamma(\mathbf{k})}\right| + \sum_{\mathbf{k},\gamma}\ln\left|1-\mathrm{e}^{-\beta Z_\gamma(\mathbf{k})}\right|,$$
$$\sum_{\omega_n}\mathrm{tr}\ln[-G'(\mathrm{i}\omega_n)]\mathrm{e}^{\mathrm{i}\omega_n\eta} = -\sum_{\alpha,\gamma}\ln\left|1-\mathrm{e}^{-\beta E'_{\alpha\gamma}}\right| + \sum_{\alpha,\gamma}\ln\left|1-\mathrm{e}^{-\beta Z'_{\alpha\gamma}}\right|, \tag{25}$$

where $E_\gamma(\mathbf{k})$ and $Z_\gamma(\mathbf{k})$ [$E'_{\alpha\gamma}$ and $Z'_{\alpha\gamma}$] denote the poles and the zeros of the Green function $G(z)$ [$G'(z)$]. By virtue of the definition of the self-energy, $Z_\gamma(\mathbf{k})$ and $Z'_{\alpha\gamma}$ correspond to the poles of the $\tilde{\Sigma}(z)$ and $\Sigma(z)$, respectively. We show in appendix C that $\tilde{\Sigma}(z)$ and $\Sigma(z)$ share the same poles, i.e. $\{Z_\gamma(\mathbf{k})\} = \{Z'_{\alpha\gamma}\}$. From equations (16), (25), we then deduce

$$\Omega_x(x') = \Omega' - \frac{1}{N}\sum_{\mathbf{k},\gamma}E_\gamma(\mathbf{k})\theta[-E_\gamma(\mathbf{k})] + \frac{1}{N}\sum_{\alpha,\gamma}E'_{\alpha\gamma}\theta[-E'_{\alpha\gamma}] \tag{26}$$

(θ is the Heaviside step function) in the zero-temperature limit. Note that the energies $E'_{\alpha\gamma}$ are N_c times degenerate, since G' is the Green function of the whole reference system (N_c clusters). Equation (26) gives the boson density

$$n = \frac{1}{N}\sum_{\mathbf{k},\gamma} \left.\frac{\partial E_\gamma(\mathbf{k})}{\partial \mu}\right|_{x'} \theta[-E_\gamma(\mathbf{k})]. \tag{27}$$

To relate n to the boson density $n_c = -\partial\Omega'/\partial\mu'$ in the reference system, we use the stationary condition $\partial\Omega_x(x')/\partial\mu' = 0$,

$$n_c = -\frac{1}{N}\sum_{\mathbf{k},\gamma} \left.\frac{\partial E_\gamma(\mathbf{k})}{\partial \mu'}\right|_{x} \theta[-E_\gamma(\mathbf{k})] + \frac{1}{N}\sum_{\alpha,\gamma} \left.\frac{\partial E'_{\alpha\gamma}}{\partial \mu'}\right|_{x} \theta[-E'_{\alpha\gamma}]. \tag{28}$$

This equation can be simplified by noting that the chemical potential μ' is a mere shift of the excitation energies $E'_{\alpha\gamma}$, so that $E'_{\alpha\gamma} + \mu'$ is independent of μ',

$$\left.\frac{\partial E'_{\alpha\gamma}}{\partial \mu'}\right|_{x} = -1. \tag{29}$$

Consider now the relation (10) between $G(z)$, $G_0(z)$ and $\tilde{\Sigma}(z)$. In this equation, $\tilde{\Sigma}(z)$ is a function of $z + \mu'$, while $G_0(z)$ and $G(z)$ are functions of $z + \mu$. It follows that $E_\gamma(\mathbf{k}) + \mu$ is a function of $\mu - \mu'$, which gives

$$\left.\frac{\partial E_\gamma(\mathbf{k})}{\partial \mu}\right|_{x'} + 1 = -\left.\frac{\partial E_\gamma(\mathbf{k})}{\partial \mu'}\right|_{x}. \tag{30}$$

From equations (27)–(30), we deduce

$$n = n_c + \frac{1}{N}\sum_{\alpha,\gamma} \theta[-E'_{\alpha\gamma}] - \frac{1}{N}\sum_{\mathbf{k},\gamma} \theta[-E_\gamma(\mathbf{k})]. \tag{31}$$

In the Mott phase, the coupling between clusters will transform the discrete excitation energies $E'_{\alpha\gamma}$ into energy bands $E_\gamma(\mathbf{k})$. Since the gap in the excitation spectrum remains nonzero, the number of negative energies cannot change, so that $n = n_c$.

Clearly, and this is confirmed by our numerical calculations, the important point here is to take the chemical potential μ' of the cluster as a variational parameter. Other parameters, such as the intersite hopping matrix $\hat{t}'$, do not have to be considered as variational in order to obtain a consistent result for the boson density. This point has also been stressed in [38].

3. Numerical results in one dimension

In this section, we present numerical results for 1D systems.

The simplest reference system consists of single-site clusters ($L = 1$). The only variational parameter is then the chemical potential $x' = \mu'$. A single-site cluster can be solved analytically exactly. The state with $p \geqslant 0$ particles is an eigenstate with the energy $\epsilon_p = -\mu' p + (U/2)p(p-1)$. This yields the partition function

$$\mathrm{e}^{-\beta\Omega'} = \sum_{p=0}^{\infty} \mathrm{e}^{-\beta\epsilon_p} \to \mathrm{e}^{-\beta\epsilon_{n_c}} \qquad (T \to 0). \tag{32}$$

The number of bosons n_c in the ground state is obtained from $\epsilon_{n_c} = \min_p \epsilon_p$. This condition leads to $n_c - 1 \leqslant \mu'/U \leqslant n_c$ if $\mu' > -U$, and $n_c = 0$ if $\mu' < 0$. In the following, we consider only the MI with one boson per site, $n = n_c = 1$, which requires $0 < \mu' < U$. The zero-temperature Green function is local in space and reads [23]

$$G'(\mathrm{i}\omega_n) = \frac{-1}{\mathrm{i}\omega_n + \mu'} + \frac{2}{\mathrm{i}\omega_n + \mu' - U}. \tag{33}$$

The self-energy $\Sigma(\mathrm{i}\omega_n) = \mathrm{i}\omega_n + \mu' - G'^{-1}(\mathrm{i}\omega_n)$ is local in real space and diagonal in reciprocal space: $\tilde{\Sigma} = \Sigma$. From equation (10) and $G_0^{-1}(k, \mathrm{i}\omega_n) = \mathrm{i}\omega_n + \mu - \epsilon_k$, we obtain

$$G(k, \mathrm{i}\omega_n) = \frac{G'(\mathrm{i}\omega_n)}{1 - (\Delta\mu' + \epsilon_k)G'(\mathrm{i}\omega_n)} = \frac{1 - z_k}{\mathrm{i}\omega_n - E_k^-} + \frac{z_k}{\mathrm{i}\omega_n - E_k^+}, \tag{34}$$

where

$$E_k^\pm = -\mu + \tfrac{1}{2}\left(-\Delta\mu' + \epsilon_k + U\right) \pm \tfrac{1}{2}\left[U^2 + 6U(\Delta\mu' + \epsilon_k) + (\Delta\mu' + \epsilon_k)^2\right]^{1/2} \tag{35}$$

and $\Delta\mu' = \mu' - \mu$. Given that $-\mu'$, $E_k^- < 0$ and $U - \mu'$, $E_k^+ > 0$ (see below), equation (26) gives

$$\Omega_x(\mu') = -2\mu' - \frac{1}{N}\sum_k E_k^-. \tag{36}$$

For $\Delta\mu' = 0$, we recover the single-site CPT results obtained earlier [19, 22, 23]. A finite $\Delta\mu'$ does not change the structure of the Green function $G(k, \mathrm{i}\omega_n)$. The excitation spectrum reveals the generic characteristics of the MI–SF transition [1]. There are two excitation branches, $E_k^+ > 0$ and $E_k^- < 0$, which coincide with the cluster excitation energies $-\mu'$ and $U - \mu'$ in the limit $t \to 0$. The dispersion of $E_k^\pm$ increases with t, which leads to a decrease of the Mott gap $E_{k=0}^+ - E_{k=0}^-$. (See, for instance, the figures in [23] for the case $\Delta\mu' = 0$.) By varying the chemical potential μ (with t and U fixed), one induces a transition from the commensurate incompressible MI to the incommensurate compressible SF when $E_{k=0}^+$ or $E_{k=0}^-$ vanishes. This transition is density driven and its critical behaviour is mean-field like. At the tip of the Mott lobe shown in figure 2, $E_{k=0}^+$ and $E_{k=0}^-$ vanish simultaneously, i.e. the Mott gap closes. This transition occurs at fixed density; it is driven by phase fluctuations and is in the universality class of the $(d + 1)$ XY model (with d the space dimension) [1].

Within the VCPT, one has to determine $\Delta\mu'$ from the stationary condition $\partial\Omega_x(\mu')/\partial\mu' = 0$,

$$\frac{1}{N}\sum_k \frac{3U + \Delta\mu' + \epsilon_k}{\left[U^2 + 6U(\Delta\mu' + \epsilon_k) + (\Delta\mu' + \epsilon_k)^2\right]^{1/2}} = 3. \tag{37}$$

Using equation (37), one can verify that the boson density $n = -\partial\Omega/\partial\mu$ obtained from equation (36) equals that of the cluster, $n = n_c = 1$, in agreement with the general proof given in section 2.4. In order for the square root in equations (35), (37) to be defined, $\Delta\mu'$ should satisfy $\Delta\mu' \leqslant D - (3 + 2\sqrt{2})U$ or $\Delta\mu' \geqslant D - (3 - 2\sqrt{2})U$, where $D = -\epsilon_{k=0} = zt$. (Note that the Mott gap vanishes when $\Delta\mu' = D - (3 \pm 2\sqrt{2})U$.) The grand potential $\Omega_x(\mu')$ is shown in figure 1 for $t/U = 0.1$. We see that the stationary point of $\Omega_x(\mu')$ is a maximum with respect to variations of μ'. This turns out to always be true regardless of the space dimension or the number of sites in the cluster. Since we expect $\Omega_x(x')$ to be a minimum with respect to other variational parameters—for instance the intracluster hopping amplitude t'—the stationary point of the grand potential $\Omega_x(x')$ will in general be a saddle point for larger clusters ($L \geqslant 2$).

Once $\Delta\mu'$ is known, the values of the chemical potential μ for which the Mott state becomes unstable are obtained from $E_{k=0}^+ = 0$ and $E_{k=0}^- = 0$. The lowest value of $\Delta\mu'$ shown in figure 1 corresponds to $\Delta\mu' = D - (3 - 2\sqrt{2})U$. As t/U increases, this value moves closer to the stationary point, and coincides with it when the Mott gap closes. This signals a transition to the superfluid state with a density $n = 1$. For larger values of t, the ground state is superfluid for any value of μ (provided the boson density remains finite).

The phase diagram of the 1D Bose–Hubbard model in figure 2 shows that the results obtained from the CPT and the VCPT differ drastically even for single-site clusters. Whereas the CPT gives the round-shaped Mott lobe characteristic of mean-field theories—and independent of the dimension but for a trivial dependence on the number z of nearest

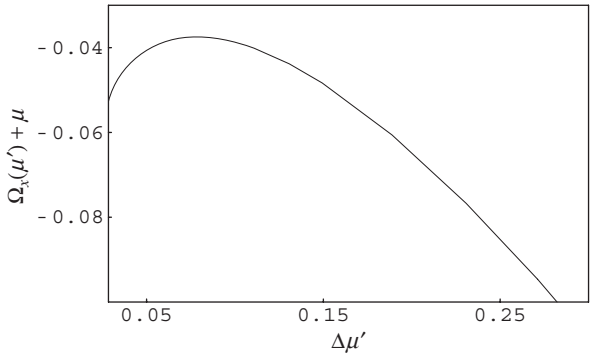

Figure 1. Grand potential $\Omega_x(\mu')$ versus $\Delta\mu' = \mu' - \mu$ in 1D for $t = 0.1$ (single-site clusters). In all figures $U = 1$.

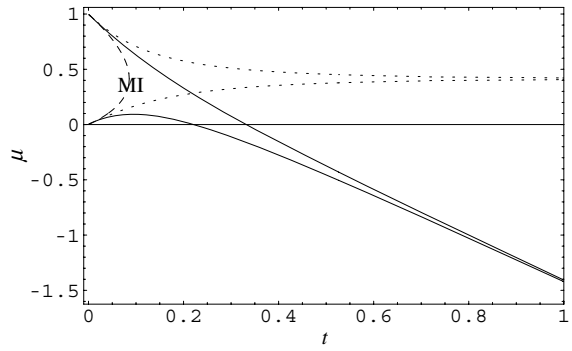

Figure 2. Phase diagram in 1D obtained from a single-site cluster. The solid lines show the boundaries between the $n = 1$ Mott insulator (MI) and the surrounding superfluid phase. The dashed line is the CPT result. The dotted lines show the values of μ' at the Mott-insulator-to-superfluid transition.

neighbours—the VCPT qualitatively reproduces the shape of the Mott lobe in 1D [9, 10, 26]. In particular, it yields a re-entrant behaviour of the MI state as t is increased with $\mu \sim 0.05U$ fixed, and a very pointed shape around the lobe tip. For sufficiently large values of t, μ' comes near $U/2$, while the decrease of μ appears to be tied to the bottom of the free boson dispersion ϵ_k, i.e. $\mu \sim -2t + \text{const}$. The gap closes very slowly as t increases, and the MI disappears for $t/U \sim 2$ (not shown in figure 2).

Note that the pointed shape of the Mott lobe in 1D is usually attributed to the slow decrease of the Mott gap,

$$E^+_{k=0} - E^-_{k=0} \sim \exp\left(-\frac{\text{const}}{\sqrt{t_c - t}}\right), \tag{38}$$

near the Berezinskii–Kosterlitz–Thouless (BKT) transition taking place at the lobe tip ($t = t_c$) [10, 26]. The fact that the single-site VCPT reproduces the correct overall shape of the Mott tip, while the physics of the BKT transition is clearly outside the reach of this method, is quite remarkable.

For larger clusters ($L \geqslant 2$), the ground state and the grand potential Ω', as well as the single-particle Green function G', can be obtained numerically using the Lanczos method [30]. The intracluster hopping amplitude $t' = t$ is held fixed, and only the chemical potential μ' is

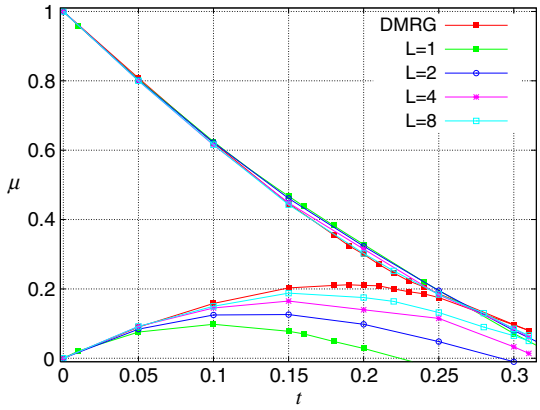

Figure 3. Phase diagram in 1D obtained from a L-site cluster. The squares show the results from the density-matrix renormalization group [10].

taken as a variational parameter. As in the case $L = 1$, the stationary point $\partial\Omega_x(\mu')/\partial\mu' = 0$ is a maximum. For a given μ, not all values of μ' are physically acceptable. On the one hand, μ' has to be such that $n_c = 1$ (we restrict ourselves to the $n = 1$ MI). On the other hand, we have to ensure that the ground state is stable. For $L = 1$, we saw that for certain values of μ', the single-particle excitation energies are complex. This instability also shows up as a disagreement between the boson density n obtained from the trace of G (equation (24)) and n_c. We use this latter criterion to verify the stability of the ground state, since it does not require us to obtain the excitation energies while minimizing the grand potential with respect to μ'.

The phase diagram of the 1D Bose–Hubbard model is shown in figure 3 together with the results obtained from the density-matrix renormalization group (DMRG) [10]. Single-site clusters give a good approximation to the upper boundary of the $n = 1$ MI. By contrast, the lower boundary obtained within the VCPT strongly depends on the number of sites in the cluster. For $L \gtrsim 8$, the VCPT reproduces fairly accurately the results obtained from the DMRG.

Figure 4 shows the spectral function $A(k, \omega) = -\pi^{-1} \operatorname{Im} G(k, \omega + \mathrm{i}\eta)$ (ω real). The spectrum consists of two well-defined dispersion branches separated by the Mott gap. We see clearly how the Mott gap closes as we move closer to the Mott lobe tip. Note that besides the two main excitation energies, the spectral function exhibits additional (weaker) structures at positive energies when the Mott gap is small (see the two bottom graphs in figure 4); we do not know whether these have a true physical meaning or are due to the finite accuracy of our numerical calculations.

As discussed in section 2, by making use of the translation-invariant self-energy $\tilde{\Sigma}$, we obtain a boson dispersion free of spurious gaps coming from the periodicity of the reference system (figure 4). This is illustrated in figure 5, where we compare the single-particle density of states $\rho(\omega) = \int (\mathrm{d}k/2\pi) A(k, \omega)$ with that obtained from the non-translation-invariant self-energy $\Sigma(k, k', z)$. In the latter case, two gaps arising from the periodicity of the four-site clusters are clearly visible.

4. Conclusion

The VCPT [32–35], which was previously applied to strongly correlated fermion systems [35–39], can be extended to boson systems. We propose a modification of the original

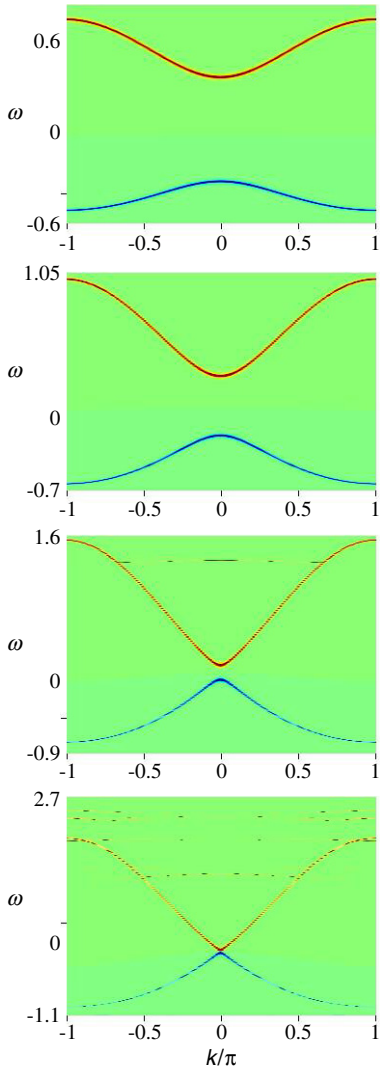

Figure 4. Spectral function $A(k, \omega) = -\pi^{-1} \operatorname{Im} G(k, \omega + \mathrm{i}\eta)$ obtained from four-site clusters: $t/U = 0.05, 0.1, 0.2$ and 0.3 (from top to bottom).

formulation which ensures that the final results are translation invariant despite the fact that the reference system breaks translation invariance. This translation-invariant VCPT is not restricted to boson systems but should also apply to fermion systems.

The results obtained for the 1D Bose–Hubbard model indicate that the VCPT is an efficient method for studying the Mott-insulator-to-superfluid transition in boson systems. We stress the importance of taking the chemical potential μ' of the cluster as a variational parameter. This ensures that the approach is thermodynamically consistent ($n = -\partial\Omega/\partial\mu = -\operatorname{Tr}(G)/(N\beta)$), and that the boson density n is the same in the system and the reference system. The grand potential is found to be a maximum with respect to variation of μ', which implies that in general it will correspond to a saddle point when several variational parameters are considered. Even

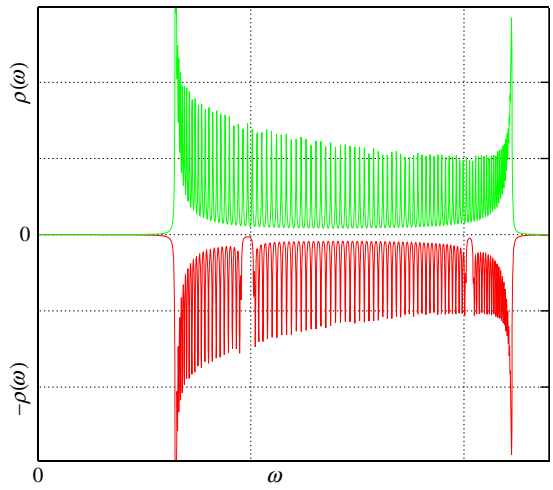

Figure 5. Comparison between the single-particle density of states ($\omega > 0$) obtained from the translation-invariant self-energy $\tilde{\Sigma}(k, z)$ (upper curve $\rho(\omega)$) with that obtained from the self-energy $\Sigma(k, k', z)$ (lower curve $-\rho(\omega)$). The plots are obtained from four-site clusters.

for one-site clusters, the VCPT and CPT—where $\mu' = \mu$ is not a variational parameter—differ drastically. Whereas the CPT gives the usual dimension-independent mean-field results, the VCPT reproduces the characteristic pointed shape and re-entrant behaviour of the Mott lobe in 1D.

The extension of our results to higher dimensions does not raise any difficulty and will be discussed elsewhere. The application of the VCPT to the superfluid phase is more subtle. In order to describe a broken gauge-symmetry phase ($\langle\psi_{\mathbf{r}}\rangle \neq 0$), one should add to the reference system Hamiltonian a field $h'_{\mathbf{r}}$ that couples to the boson operator $\psi_{\mathbf{r}}$. The set x' of variational parameters will therefore at least include the chemical potential μ' and the field h'. A finite value of h' at the stationary point implies a nonzero condensate $\langle\psi_{\mathbf{r}}\rangle$ and superfluidity. Whether or not the VCPT will satisfy the Hugenholz–Pines theorem and thus correctly describe the gapless Bogoliubov sound mode should determine the applicability of the VCPT to the superfluid phase.

Acknowledgment

WK thanks the EPSRC for support through the grant GR/S18571/01.

Appendix A. Derivation of equation (19)

Let us consider the integral

$$I = \oint \frac{\mathrm{d}z}{2\mathrm{i}\pi} n_{\mathrm{B}}(z)\,\mathrm{tr}_c \ln\left(1 - \frac{\Delta h_0(\mathbf{K})}{z - y}\right)\mathrm{e}^{z\eta} = \oint \frac{\mathrm{d}z}{2\mathrm{i}\pi} n_{\mathrm{B}}(z) \sum_{\alpha=1}^{L} \ln\left(1 - \frac{\lambda_\alpha(\mathbf{K})}{z - y}\right)\mathrm{e}^{z\eta}, \qquad \text{(A.1)}$$

where $\lambda_\alpha(\mathbf{K})$ ($\alpha \in [1, L]$) are the eigenvalues of $\Delta h_0(\mathbf{K})$. $n_{\mathrm{B}}(z) = (\mathrm{e}^{\beta z} - 1)^{-1}$ is the Bose–Einstein distribution function. If we choose $y > \max_{\alpha,\mathbf{K}} |\lambda_\alpha(\mathbf{K})|$, the branch cut of the logarithm in equation (A.1) does not extend to the origin $z = 0$, and we can evaluate I

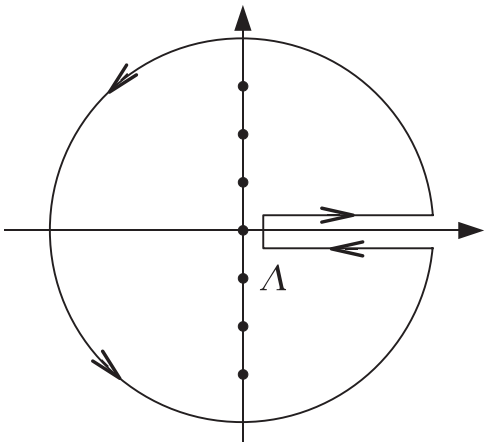

Figure A.1. Integration contour used in equation (A.1). The black dots denote the bosonic Matsubara frequencies $\mathrm{i}\omega_n$.

using the contour shown in figure A.1 where $0 < \Lambda \leqslant y - \max_{\alpha,\mathbf{K}} |\lambda_\alpha(\mathbf{K})|$. From the residue theorem, we then obtain

$$I = \frac{1}{\beta}\sum_{\alpha,\omega_n} \ln\left(1 - \frac{\lambda_\alpha(\mathbf{K})}{\mathrm{i}\omega_n - y}\right) \mathrm{e}^{\mathrm{i}\omega_n \eta} = \int_\Lambda^\infty \frac{\mathrm{d}\epsilon}{2\mathrm{i}\pi} n_\mathrm{B}(\epsilon) \sum_{\alpha=1}^{L} \left[\ln\left(1 - \frac{\lambda_\alpha(\mathbf{K})}{\epsilon + \mathrm{i}\eta - y}\right) - \text{c.c.}\right]. \tag{A.2}$$

The factor $n_\mathrm{B}(z)\mathrm{e}^{z\eta}$ ensures that the part of the contour at infinity does not contribute to the integral. An integration by parts gives

$$\begin{aligned} I &= -\int_\Lambda^\infty \frac{\mathrm{d}\epsilon}{2\mathrm{i}\pi} \frac{1}{\beta} \ln\left(1 - \mathrm{e}^{-\beta\epsilon}\right) \sum_{\alpha=1}^{L} \frac{\partial}{\partial\epsilon} \left[\ln\left(1 - \frac{\lambda_\alpha(\mathbf{K})}{\epsilon + \mathrm{i}\eta - y}\right) - \text{c.c.}\right] \\ &= \frac{1}{\beta}\sum_{\alpha=1}^{L} \ln\left(1 - \mathrm{e}^{-\beta(y+\lambda_\alpha(\mathbf{K}))}\right) - \frac{L}{\beta}\ln\left(1 - \mathrm{e}^{-\beta y}\right). \end{aligned} \tag{A.3}$$

Equation (19) follows from (A.2) and (A.3).

Appendix B. Derivation of equations (25)

Let us consider the integral

$$I = \oint \frac{\mathrm{d}z}{2\mathrm{i}\pi} n_\mathrm{B}(z)\,\mathrm{tr}\ln[-G'(z)]\mathrm{e}^{z\eta} = \oint \frac{\mathrm{d}z}{2\mathrm{i}\pi} n_\mathrm{B}(z) \sum_{\alpha=1}^{L} \ln[-G'_\alpha(z)]\mathrm{e}^{z\eta}, \tag{B.1}$$

where $G'_\alpha(z)$ ($\alpha \in [1, L]$) are the eigenvalues of $G'(z)$. The (exact) bosonic Green function can be written as a sum of simple poles,

$$G'_\alpha(z) = \sum_\gamma \frac{r_{\alpha\gamma}}{z - E'_{\alpha\gamma}}, \tag{B.2}$$

where $\mathrm{sgn}(r_{\alpha\gamma}) = \mathrm{sgn}(E'_{\alpha\gamma})$. The excitation energies $E'_{\alpha\gamma}$ are nonzero in the Mott phase. As a result

$$-G'_\alpha(z=0) = \sum_\gamma \frac{r_{\alpha\gamma}}{E'_{\alpha\gamma}} > 0 \tag{B.3}$$

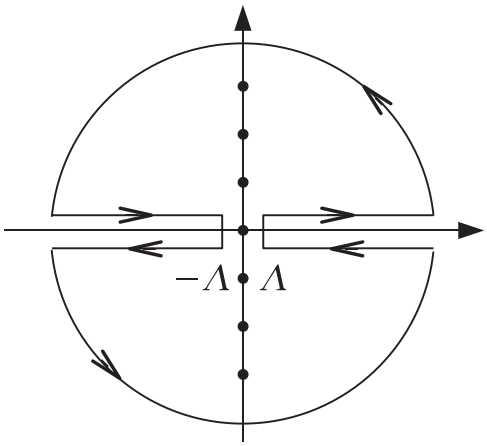

Figure B.1. Integration contour used in equation (B.1).

and the branch cut of the logarithm in equation (B.1) does not extend to the origin. We can therefore evaluate I using the contour shown in figure B.1,

$$\begin{aligned} I &= \frac{1}{\beta}\sum_{\alpha,\omega_n} \ln[-G'_\alpha(\mathrm{i}\omega_n)]\mathrm{e}^{\mathrm{i}\omega_n\eta} \\ &= \left(\int_\Lambda^\infty + \int_{-\infty}^{-\Lambda}\right)\frac{\mathrm{d}\epsilon}{2\mathrm{i}\pi} n_\mathrm{B}(\epsilon)\sum_\alpha \left\{\ln[-G'_\alpha(\epsilon+\mathrm{i}\eta)] - \mathrm{c.c.}\right\} \\ &= -\left(\int_\Lambda^\infty + \int_{-\infty}^{-\Lambda}\right)\frac{\mathrm{d}\epsilon}{2\mathrm{i}\pi}\frac{1}{\beta}\ln\left|1-\mathrm{e}^{-\beta\epsilon}\right| \\ &\quad\times \sum_\alpha [G'^{-1}_\alpha(\epsilon+\mathrm{i}\eta)\partial_\epsilon G'_\alpha(\epsilon+\mathrm{i}\eta) - \mathrm{c.c.}], \end{aligned} \tag{B.4}$$

where $0 < \Lambda < \min_{\alpha,\gamma}(|E'_{\alpha\gamma}|, |Z'_{\alpha\gamma}|)$, with $Z'_{\alpha\gamma}$ the zeros of $G'(z)$. The last line in (B.4) is obtained by integrating by parts. The factor inside the last brackets vanishes unless ϵ is near a pole or a zero of $G'_\alpha(\epsilon)$. Near a pole, $G'_\alpha(\epsilon) \simeq r_{\alpha\gamma}/(\epsilon+\mathrm{i}\eta-E'_{\alpha\gamma})$, and $[\cdots] = 2\mathrm{i}\pi\,\delta(\epsilon-E'_{\alpha\gamma})$. The zeros of $G'_\alpha(z)$ are given by the poles of the self-energy $\Sigma(z)$, which shares the same analytical properties as $G'(z)$ and can therefore be written as a sum of simple poles as in equation (B.2) (see appendix C for a more detailed discussion). It follows that $G'_\alpha(z)$ has only simple zeros $Z'_{\alpha\gamma}$ and can be approximated by $G'_\alpha(z) \simeq s_{\alpha\gamma}(z - Z'_{\alpha\gamma})$ near $z = Z'_{\alpha\gamma}$. The factor inside the brackets in equation (B.4) then gives $-2\mathrm{i}\pi\,\delta(\epsilon - Z'_{\alpha\gamma})$. We deduce

$$I = -\frac{1}{\beta}\sum_{\alpha,\gamma}\ln\left|1-\mathrm{e}^{-\beta E'_{\alpha\gamma}}\right| + \frac{1}{\beta}\sum_{\alpha,\gamma}\ln\left|1-\mathrm{e}^{-\beta Z'_{\alpha\gamma}}\right|. \tag{B.5}$$

The second of equations (25) follows from (B.4) and (B.5). The first one can be derived similarly. Analogous results for fermionic systems can be found in [33].

Appendix C. Cluster self-energy $\Sigma(z)$

In this appendix, we discuss two important properties of the cluster self-energy $\Sigma(z)$.

C.1. $\lim_{|z|\to\infty} \Sigma(z)$

The cluster self-energy $\Sigma(z)$ tends to a constant value equal to the Hartree–Fock value $2Un$ when $|z| \to \infty$. A similar result holds for the fermionic Hubbard model: see for instance appendix A in [43]; the derivation given in this paper can be straightforwardly extended to the Bose–Hubbard model.

C.2. Poles of $\Sigma(z)$ *and* $\tilde{\Sigma}(z)$

The (matrix) self-energy $\Sigma(z)$ shares the same analytical properties as the Green function $G'(z)$. Its Lehmann representation

$$\Sigma(z) = \Sigma(\infty) + \sum_{\alpha,\gamma} |\alpha, \gamma\rangle \frac{q_{\alpha\gamma}}{z - Z_{\alpha\gamma}} \langle\alpha, \gamma| \tag{C.1}$$

(we use a bra-ket notation) leads to

$$\tilde{\Sigma}(\mathbf{k}, z) = \langle\mathbf{k}|\Sigma(z)|\mathbf{k}\rangle = \Sigma(\infty) + \sum_{\alpha,\gamma} |\langle\mathbf{k}|\alpha, \gamma\rangle|^2 \frac{q_{\alpha\gamma}}{z - Z_{\alpha\gamma}}, \tag{C.2}$$

where $\Sigma(\infty) = 2Un$. Since both $\{|\mathbf{k}\rangle\}$ and $\{|\alpha, \gamma\rangle\}$ span the whole Hilbert space, $\langle\mathbf{k}|\alpha, \gamma\rangle$ cannot vanish for all $\mathbf{k}$. This implies that all poles $Z_{\alpha\gamma}$ of $\Sigma(z)$ also show up as poles of $\tilde{\Sigma}(z)$.

References

[1] Fisher M P A, Weichman P B, Grinstein G and Fisher D S 1989 *Phys. Rev.* B **40** 546
[2] Jaksch D, Bruder C, Cirac J I, Gardiner C W and Zoller P 1998 *Phys. Rev. Lett.* **81** 3108
[3] Greiner M, Mandel O, Esslinger T, Hänsch T W and Bloch I 2002 *Nature* **415** 39
[4] Stöferle T, Moritz H, Schori C, Köhl M and Esslinger T 2004 *Phys. Rev. Lett.* **92** 130403
[5] Gerbier F, Widera A, Fölling S, Mandel O, Gericke T and Bloch I 2005 *Phys. Rev. Lett.* **95** 050404
[6] Rokhsar D S and Kotliar B G 1991 *Phys. Rev.* B **44** 10328
[7] Krauth W, Caffarel M and Bouchaud J-P 1992 *Phys. Rev.* B **45** 3137
[8] Schroll C, Manquardt F and Bruder C 2004 *Phys. Rev.* A **70** 053609
[9] Kühner T D and Monien H 1998 *Phys. Rev.* B **58** R14741
[10] Kühner T D, White S R and Monien H 2000 *Phys. Rev.* B **61** 12474
[11] Roth R and Burnett K 2003 *Phys. Rev.* A **67** 031602(R)
[12] Roth R and Burnett K 2003 *Phys. Rev.* A **68** 023604
[13] Batrouni G G, Scalettar R T and Zimanyi G T 1992 *Phys. Rev. Lett.* **65** 1765
[14] Batrouni G G and Scalettar R T 1992 *Phys. Rev.* B **46** 9051
[15] Krauth W and Trivedi N 1991 *Europhys. Lett.* **14** 627
[16] Wessel S, Alet F, Troyer M and Batrouni G G 2004 *Phys. Rev.* A **70** 053615
[17] Sheshadri K, Krishnamurthy H R, Pandit R and Ramakrishnan T V 1993 *Europhys. Lett.* **22** 257
[18] Kampf A P and Zimanyi G T 1993 *Phys. Rev.* B **47** 279
[19] van Oosten D, van der Straten P and Stoof H T C 2001 *Phys. Rev.* A **63** 053601
[20] Sachdev S 1999 *Quantum Phase Transitions* (Cambridge: Cambridge University)
[21] Dickerscheid D B M, van Oosten D, Denteneer P J H and Stoof H T C 2003 *Phys. Rev.* A **68** 043623
[22] Konabe S, Nikuni T and Nakamura M 2006 *Phys. Rev.* A **73** 033621
[23] Sengupta K and Dupuis N 2005 *Phys. Rev.* A **71** 033629
[24] Freericks J K and Monien H 1994 *Europhys. Lett.* **26** 545
[25] Freericks J K and Monien H 1996 *Phys. Rev.* B **53** 2691
[26] Elstner N and Monien H 1999 *Phys. Rev.* B **59** 12184
[27] Buonsante P and Vezzani A 2005 *Phys. Rev.* A **72** 013614
[28] Gros C and Valentí R 1993 *Phys. Rev.* B **48** 418
[29] Sénéchal D, Pérez D and Pioro-Ladrière M 2000 *Phys. Rev. Lett.* **84** 522
[30] Sénéchal D, Perez D and Plouffe D 2002 *Phys. Rev.* B **66** 075129
[31] Hubbard J 1963 *Proc. R. Soc.* A **276** 238
[32] Potthoff M 2003 *Eur. Phys. J.* B **32** 429

[33] Potthoff M 2003 *Eur. Phys. J.* B **36** 335
[34] Potthoff M, Aichhorn M and Dahnken C 2003 *Phys. Rev. Lett.* **91** 206402
[35] Dahnken C, Aichhorn M, Hanke W, Arrigoni E and Potthoff M 2004 *Phys. Rev.* B **70** 245110
[36] Aichhorn M, Evertz H G, von der Linden W and Potthoff M 2004 *Phys. Rev.* B **70** 235107
[37] Sénéchal D, Lavertu P-L, Marois M-A and Tremblay A-M S 2005 *Phys. Rev. Lett.* **94** 156404
[38] Aichhorn M and Arrigoni E 2006 *Europhys. Lett.* at press
(Aichhorn M and Arrigoni E 2005 *Preprint* cond-mat/0502047)
[39] Dahnken C, Potthoff M, Arrigoni E and Hanke W 2005 *Preprint* cond-mat/0504618
[40] Luttinger J M and Ward J C 1960 *Phys. Rev.* **118** 1417
[41] De Dominicis C and Martin P C 1964 *J. Math. Phys.* **5** 14
[42] De Dominicis C and Martin P C 1964 *J. Math. Phys.* **5** 31
[43] Vilk Y and Tremblay A-M S 1997 *J. Physique* I **7** 1309